Relocalization in Floppy Free Radicals: Ab Initio Calculations of the C_3H_3O Isomers

A. L. Cooksy

Department of Chemistry, University of Mississippi, University, Mississippi 38677

Received: December 18, 1997; In Final Form: April 15, 1998

Several isomers with molecular formula C_3H_3O may exhibit unusual properties by virtue of a configurational isomerization pathway that changes the localization of an unpaired electron. A series of ab initio calculations was undertaken at the UHF, B3LYP, MCSCF, and QCISD levels with the 6-311G(d,p) basis set to ascertain the geometries, relative energies, isomerization barriers, and relevant spectroscopic properties of the lowest energy structural and configurational C_3H_3O isomers. The most stable structures, with QCISD relative energies (kJ mol^{-1}) of the stable configurations given in parentheses, are H_2C_2HCO (0, 8, 8), H_3C_3O (47), H_2C_3HO (87, 100), and HC_2HCHO (94, 95, 101, 107). The H_2C_2HCO and H_2C_3HO structures are found to have distinct isomers connected by relocalization pathways. The H_3C_3O structure possesses two favorable canonical geometries, but the single optimized structure is an average of these. Potential surfaces have been calculated along two vibrational bending coordinates for H_2C_2HCO and H_2C_3HO and along a single bending coordinate for H_3C_3O. Extremely large amplitude bending motions are predicted for these three lowest energy structures, and at typical combustion temperatures it is likely that these molecules exist effectively as admixtures of two or more canonical structures.

1. Introduction

A molecule with an unpaired electron conjugated with a π bond may have two or more relatively stable canonical forms for the same structural isomer. The HC_3O radical, for example, may be depicted as either $H-\dot{C}_a\equiv C_b-\dot{C}_c=O$ (I) or as $H-\dot{C}_a=C_b=C_c=O$ (II). In the first case, the σ bonding orbitals of the C_c atom are essentially sp^2 hybrids and those of the C_a atom are sp. In the second case, the hybrid orbital assignments are reversed. The effect of multiple, proximate, stable canonical structures is apparent on the ab initio vibrational potential energy surfaces of HC_3O and several isovalent molecular free radicals.[1−3] The surfaces exhibit extremely flat bending potential energy surfaces, in some cases with zero-point bond angle oscillations likely to extend over 40°. Two or more minima, corresponding to distinct canonical forms, have been identified on several of these ab initio surfaces. No bonds are broken during interconversion between these structures, and hence the isomerization barriers are less than 20 kJ mol^{-1}.

The chemical structure and activity of the molecule is more profoundly altered by this form of isomerization than by other low-barrier isomerizations such as hindered internal rotation. This report differentiates among isomeric groups as follows: structural isomers differ in the sequence of the chemical bonds (e.g., HCCH vs H_2CC); configurational isomers share the same structure but differ in chemically-significant bond orientations and rearrangements (e.g., *cis*- and *trans*-1,2-difluoroethene). The low-energy isomerization between configurations that results from redistribution of the unpaired electron density in a free radical, as in HC_3O, we shall call a "relocalization".

The facile interconversion of a structure among several distinct configurations by relocalization forebodes unexpectedly complex reaction dynamics, at thermal energies greater than 1000 K. This is particularly relevant for the hydrocarbon and oxyhydrocarbon radicals, many of which are crucial intermediates in the combustion chemistry of hydrocarbon fuels.

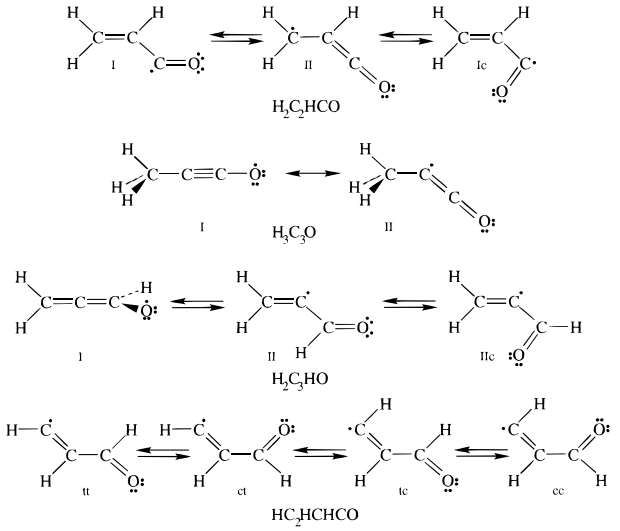

Figure 1. Canonical structures of the lowest energy C_3H_3O isomers investigated in this work.

The C_3H_3O isomers provide illustrations of relocalization pathways that differ appreciably from the HC_3O systems. Figure 1 shows those canonical structures expected to be the most stable for this molecular formula. The H_2C_2HCO structure has three configurations shown: the *cis* and *trans* forms of 3-propenalyl (I and Ic), with the electron in an in-plane sp^2 hybrid orbital, and 3-propenonyl (II), with the unpaired electron in an out-of-plane *p*-type orbital. The H_2C_3HO structure is also shown with three configurations: propadienoxy (I), with an allene-like nonplanar geometry, and the *cis* and *trans* forms of 2-propenalyl (II and IIc), with planar geometries. For H_3C_3O, two canonical forms can be drawn: the 1-propynoxy (I) and the 2-propenonyl (II). All of these relocalizations result from the exchange of an unpaired electron and a π bonding pair in the canonical structure. A fourth structure, HC_2HCHO or 1-propenalyl, does

S1089-5639(98)00566-0 CCC: $15.00
Published on Web 06/05/1998

not have distinct relocalization configurations but does have several *cis*−*trans* isomers.

The primary goal of the present work has been to find the extent to which these molecules will be subject to the same large-amplitude motion and multiple minima observed in the HC_3O series. A secondary goal is the determination of the relative energies of the most stable isomers of this chemical formula. Although ab initio studies of the $C_3H_3O^+$ isomers[4,5] have been reported, there appear to be no previously published studies of the charge-neutral compounds.

These studies may also prove relevant to the interstellar chemistry of the C_3H_3O isomers and the chemistry of acrolein and methylketene. Propynal (H_2CCCHO) and proadienone (CCCO) have both been observed by radio astronomy of interstellar molecular clouds.[6] Both of these molecules have been postulated to be formed by dissociative recombination of $H_3C_3O^+$.[7−9] The pathways for this dissociation will depend on the structures and vibrational potential energy surface of the neutral molecule. Hydrogen abstraction of acrolein by radical chemistry or photolysis should kinetically favor the H_2C_2HCO, H_2C_3HO, or HC_2HCHO structural isomers investigated in this work, while H_2C_2HCO or H_3C_3O may be formed by hydrogen abstraction from methylketene. Ensuing reaction pathways will be determined by the stability, structure, and prospects for relocalization of these radical intermediates.

2. Methods

The multiconfiguration self-consistent field (MCSCF) calculations described here were carried out using the program Gamess 5.4;[10] all other calculations employed Gaussian 94.[11] The results cited in this work are obtained with a 6-311G(d,p) basis set[12,13] unless otherwise indicated. That the basis set is well-converged at this size is manifest in previous studies of HC_3O and similar molecules.[2,3] Analytical geometry optimizations were carried out from initial geometries corresponding to each of the structures in Figure 1.

Configuration interaction (CI) calculations on this series of molecules must be undertaken with care, because the conjugated π electron systems may be poorly represented by wave functions constructed from single and double substitutions of a single Hartree−Fock reference. We therefore carried out MCSCF geometry optimizations[14] for configurations of the three lowest energy structures. A (9,9) complete active space (nine electrons in nine molecular orbitals) was used to test the reliability of the geometries and relative energies calculated using the single reference methods. This active space allows inclusion of all electrons not identified specifically with the 1s electron cores or the σ bonding system. For the lowest energy structures, MCSCF(11,10) and MCSCF(11,11) calculations were used to test convergence with respect to size of the active space.

Energies calculated at the MCSCF(9,9) level were quite sensitive to selection of the active space orbitals. Orbitals were prepared both by standard Hartree−Fock methods and by use of Pipek−Mezey localization[15] to simplify selection of the occupied orbitals. Active spaces were chosen by calculating unrestricted Hartree−Fock (UHF) basis eigenvectors at the quadratic configuration interaction with single and double substitutions (QCISD) optimized geometry and then selecting those orbitals from the eight highest occupied and five lowest unoccupied UHF orbitals that yielded the lowest energy at the QCISD geometry. The MCSCF(9,9) optimized geometry was in each case sufficiently similar to the QCISD geometry that a shift of less than 3 mhar in the absolute energy was observed after optimization. In tests on over 30 active spaces, those that yielded the lowest energies at the QCISD geometry also yielded the lowest energies at the MCSCF optimized geometry.

Previous calculations[2,3] showed that QCISD and MCSCF give energies and geometries for the HC_3O isovalent series very similar to those obtained by coupled cluster and Møller−Plesset perturbation theory methods. The quadratic term in QCISD is added into the normal configuration interaction expansion in order to obtain a size-consistent, rather than variational, method.[16] Although size-consistency is not an issue in these single molecule calculations, comparison to experimental data on the ground state of HC_3O found the geometry, hyperfine parameters, and the one observed vibrational frequency predicted at the QCISD level to be superior to those obtained by CISD.[2] Single-point energy calculations at the QCISD optimized geometries have also been carried out with the CCSD(T)[16] and MP4(SDTQ)[17] methods to test consistency of the energy calculation among different approximations.

The rapid rise in popularity of density functional methods mandates our testing these methods on the present systems as well. Geometry optimizations were therefore carried out with the B3LYP Hamiltonian, the hybrid three-parameter functional of Becke[18] incorporating the correlation functional of Lee, Yang, and Parr.[19]

Harmonic vibrational frequencies were calculated at the QCISD/6-311G(d,p) level for the six most stable configurations of C_3H_3O and for transition states of the H_2C_2HCO I ⇌ II, H_2C_2-HCO I ⇌ Ic, and H_2C_3HO I ⇌ II isomerizations. The transition state frequencies allow correction of the isomerization barriers for zero-point energy contributions from the perpendicular vibrational coordinates.[2,20] The bending frequencies in the harmonic calculations are likely to be especially inaccurate given the considerable anharmonicity of the isomerization coordinates. However, the lowest frequency modes also have the least impact on the overall zero-point energy.

The low-frequency anharmonicities are nonetheless important for predicting spectroscopic frequencies. The structure of the vibrational potential energy surface along two local coordinates was therefore obtained for H_2C_2HCO and H_2C_3HO by a series of geometry optimizations with those coordinates fixed: the CCO angle and CCCO dihedral angle for H_2C_2HCO; the CCO angle and HCCO dihedral angle for H_2C_3HO. QCISD energies were determined for 56 points on the H_2C_2HCO surface and 38 on the H_2C_3HO surface. These points were least-squares fit to two-dimensional polynomial-plus-Gaussian functions to a standard deviation of less than 20 cm^{-1} for plotting. QCISD energies were chosen over MCSCF for these surfaces to avoid the difficulty of maintaining suitable active spaces throughout a large range of intermediate geometries.

Such effective potential energy surfaces are informative only to the extent that the coordinates chosen are decoupled from the remaining coordinates. The displacement vectors calculated at the potential minima of H_2C_2HCO support this approximation, but configuration II of H_2C_3HO has several a″ modes which contribute appreciably to the HCCO dihedral motion. It is hopeful that significantly improved predictions of the lowest bending frequencies may be obtained by calculating two-dimensional vibrational wave functions on these surfaces.

3. Results and Discussion

3.1. Relative Energies and Comparison of Methods. The QCISD optimized geometries are drawn in Figure 2. Table 1 lists the energies of the most stable C_3H_3O local minima found, calculated relative to the H_2C_2HCO I configuration at various levels of theory. All structures tested at the QCISD level

TABLE 1: Ab Initio Energies (kJ mol^{-1}) of Selected H_3C_{30} Structural and Configurational Isomers Relative to the H_2C_2HCO I Structure[a]

	UHF	B3LYP	CISD	MCSCF(9,9)	QCISD	CCSD(T)	MP4(SDTQ)
H_2C_2HCO I	0.0	0.0	0.0	0.0	0.0	0.0	0.0
H_2C_2HCO II	−1.9	−8.3	0.8	24.1	7.6	9.3	4.2
H_2C_2HCO Ic	8.1	10.2	9.1	6.7	8.0	8.1	10.0
H_3C_3O	41.7	27.6	41.8	48.0	47.1	47.7	41.4
H_2C_3HO I	59.9	71.4	92.5	105.1	86.8	90.0	124.7
H_2C_3HO II	63.7	96.1	102.5	91.3	99.6	100.7	134.5
HC_2HCHO tt	57.6	95.3	95.3	87.3	94.3	96.2	126.5
HC_2HCHO tc	59.7	95.7	97.6	89.0	95.4	97.0	128.2
HC_2HCHO cc	64.3	103.3	103.7	94.3	101.4	103.4	134.7
HC_2HCHO ct	68.5	108.9	108.6	97.8	106.5	108.6	140.9

[a] CCSD(T) and MP4(SDTQ) energies are evaluated at the QCISD optimized geometry. The basis set is 6-311G(d,p) for all listed results. Agreement of MCSCF energies for H_2C_2HCO II and H_2C_3HO I improved at higher active space (see text).

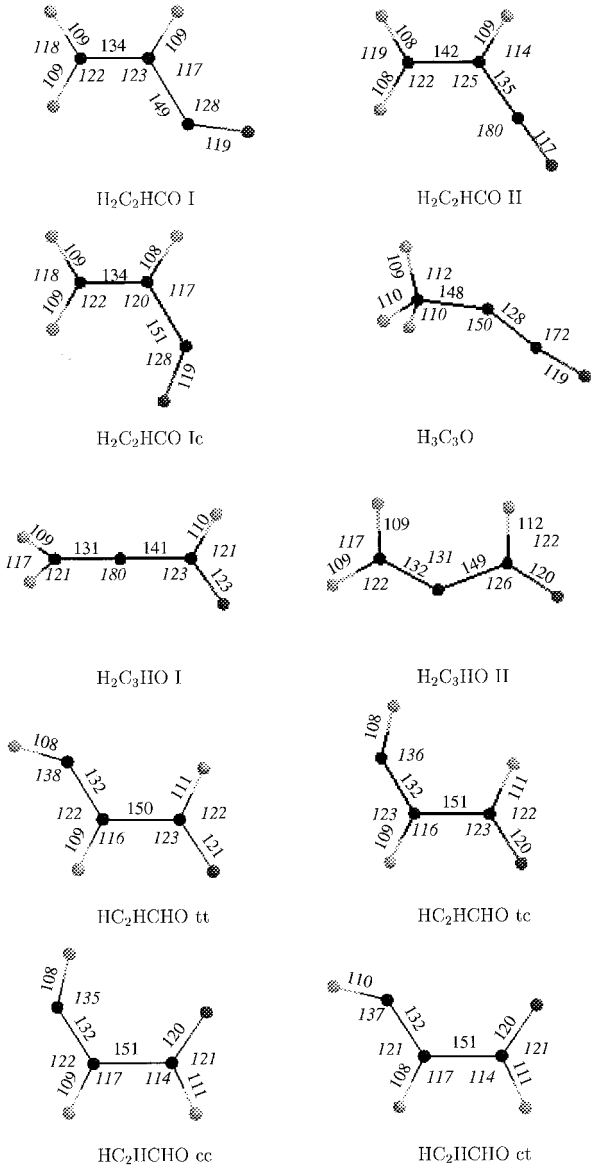

Figure 2. QICSD/6-311G(d,p) optimized geometries of the most stable C_3H_3O isomers. Bond lengths are in picometers, and angles (in italics) are in degrees.

converged to C_s symmetric forms. The H_2C_2HCO II, H_2C_3HO I, and H_3C_3O configurations are found to have $^2A''$ ground electronic states; all others have $2A'$ ground states. The most stable structural isomer of the neutral molecule is H_2C_2HCO, followed by H_3C_3O, H_2C_3HO, and HC_2HCHO. As found for HC_3O, the QCISD and CCSD(T) energies are consistent to within about 3 kJ mol^{-1}. However, in the present work this degree of reproducibility is still insufficient to assign the energy ordering of some configurations. For example, configuration II of H_2C_2HCO is more stable than Ic by 0.4 kJ mol^{-1} at the QCISD level but less stable by 1.2 kJ mol^{-1} at the CCSD(T) level.

As found for HC_3O, the present UHF relative energies are lower than those predicted by the correlated methods. The UHF energy ordering of the C_3H_3O configurations is similar to that seen at higher levels of theory, but there are two major differences: (i) at the UHF level, the lowest energy configuration of all is predicted to be H_2C_2HCO II rather than H_2C_2-HCO I; (ii) at their most stable configurations, HC_2HCHO is predicted to be more stable than H_2C_3HO at UHF, and vice versa at higher levels. These significant qualitative disagreements are the results of relative energy shifts of only about 10 kJ mol^{-1}, but these are the same magnitude as the relative energies themselves.

The higher energy QCISD calculations are indeed spin-contaminated. All of the species in this study have doublet spin ground states and an ideal value of $\langle S^2 \rangle$ of 0.75. Prior to annihilation of the spin contaminant, $\langle S^2 \rangle$ in the single-reference calculations ranges between 0.83 and 0.89 for the two lowest energy structures (consistent with values observed for HC_3O) but extends to between 1.10 and 1.16 for all configurations of H_2C_3HO and HC_2HCHO. Annihilation reduces these values to between 0.75 and 0.84.

The MCSCF calculations, on the other hand, are immune to spin contamination but suffer from under sampling of the single and double substitutions. Absolute energies calculated by the variational CISD method are lower than the MCSCF values by more than 0.35 hartree, whereas the CISD, QCISD, CCSD(T), and MP4(SDTQ) absolute energies all lie within 0.11 hartree for any given structure. Indications from the MCSCF results are that high-order substitutions are not crucial to these wave functions. Although the contribution from the UHF reference wave function was often quite small ($c_0 = 0.68$ for H_2C_3HO II), the UHF reference wave function and its single and double substitutions accounted for at least 94% of the final MCSCF wave function in all cases.

The relative merits of the MCSCF and QCISD techniques are therefore debatable in application to these systems, yet neither drawback is so severe as to impact the principal results. The MCSCF(9,9) geometries are consistent with the QCISD geometries to within 0.020 Å for bond lengths and 1.5° for bond angles, with two exceptions. The H_2C_3HO I CCC bond angle is larger by 5.6° at the QCISD level than at the MCSCF level, and the CCC bond angle in H_3C_3O is smaller by 6.7° at QCISD than at MCSCF. The flatness of the vibrational potentials along the CCC bending coordinates in both of these molecules makes

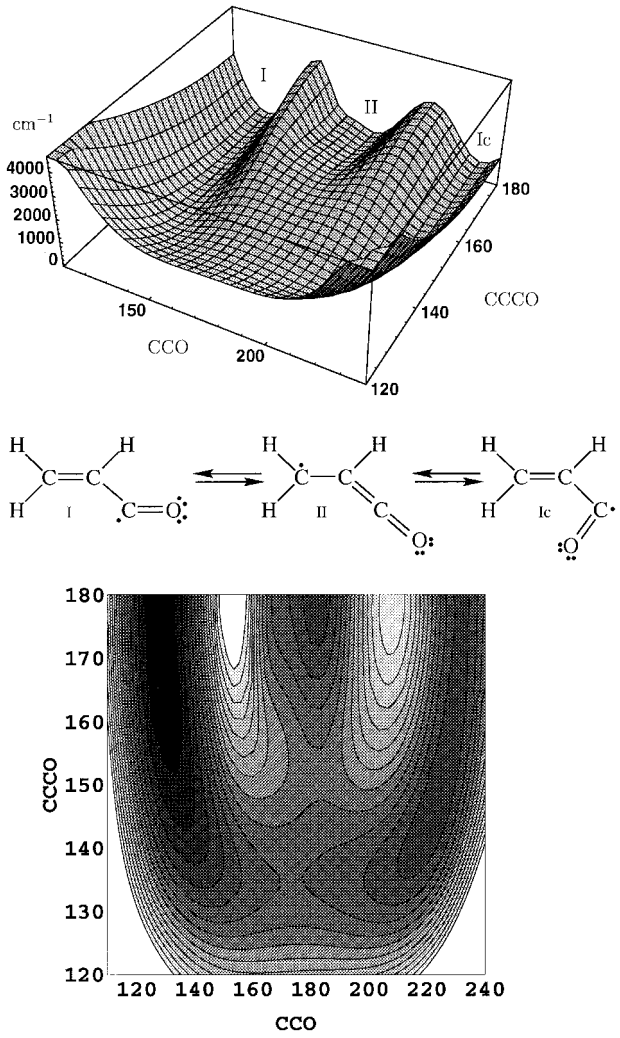

Figure 3. Contour and perspective plots of the effective vibrational potential energy surface of H_2C_2HCO as a function of the CCO bond angle and CCCO dihedral angle. Contours are at 200 cm^{-1} intervals, and darker regions indicate lower energy.

these discrepancies unsurprising and restricts their impact on the relative energies.

In fact, QCISD and MCSCF(9,9) relative energies agree to within 3 kJ mol^{-1} for configurations within a given structural isomer, with two critical exceptions. At the QCISD level, the H_2C_2HCO II energy relative to H_2C_2HCO I is 7.6 kJ mol^{-1}, and the H_2C_3HO II energy relative to H_2C_3HO I is 12.8 kJ mol^{-1}. At the MCSCF(9,9) level, these energies are predicted to be 24.1 and -13.8 kJ mol^{-1}, respectively. This discrepancy is principally attributable to poor convergence of the active space for the two A″ states, H_2C_2HCO II and H_2C_3HO I. Extension of the MCSCF active space to (11,11) improves agreement with the QCISD results, bringing these two relative energies to 13.8 and 9.6 kJ mol^{-1}, respectively.

The B3LYP calculations gave excellent agreement with the more expensive QCISD results for geometries and relative energies of the HC_2HCHO configurational isomers but poorer agreement in other cases. The relative energies in Table 1 exemplify these comparisons: the B3LYP energies of the H_2C_2-HCO II and H_3C_3O configurations relative to H_2C_2HCO I are lower than the corresponding QCISD energies by 16 and 20 kJ mol^{-1}, respectively. In the case of the H_2C_2HCO isomers this leads to a dramatic shift in the relative stability of the lowest energy configurations.

TABLE 2: Selected ab Initio Harmonic Vibrational Frequencies (cm^{-1}) and Infrared Intensities (km mol^{-1}) for the Most Stable C_3H_3O Isomers[a]

H_2C_2HCO I			H_2C_2HCO II			H_2C_2HCO Ic		
a″	142	0.02	a′	225	3.0	a″	28	0.02
a′	311	2.3	a″	344	0.1	a′	278	2.8
a′	545	3.9	a″	361	23.7	a″	567	3.4
a′	1915	210.9	a″	451	29.5	a′	1904	117.6
			a″	687	52.4			
			a′	2183	542.4			
H_3C_3O			H_2C_3HO I			H_2C_3HO II		
a″	90	20.4	a″	94	5.3	a″	87	1.2
a′	172	10.8	a′	213	4.1	a″	253	2.8
a″	417	181.8	a″	426	4.6	a″	471	1.7
a′	520	13.8	a′	942	75.4	a′	563	2.3
a″	622	143.9	a′	1527	77.0	a′	1881	310.9
a′	2131	298.4	a′	3027	67.0	a′	2888	91.3

[a] Frequencies selected are those below 600 cm^{-1} and any with intensities greater than 50 km mol^{-1}.

Having experimental data for HC_3O that is lacking for the present compounds, we also carried out B3LYP/6-311(d,p) calculations on HC_3O. Our results suggest that, for these relocalization problems, it remains necessary to rely on more time-intensive methods such as QCISD and MCSCF. The cumulenic form II of HC_3O is predicted by B3LYP to be more stable than the acetylenic configuration I by 6 kJ mol^{-1}, yet configuration I is the experimentally observed form. Other B3LYP parameters of configuration I are also inconsistent with the experimental results, predicting a CCO bond angle of 146.8° and a $^{13}C_c$ Fermi contact term of 249 MHz; the experimental values are 136.5(6)° and 347.6(3.2) MHz, respectively. The QCISD values, 133.3° and 378 MHz, are in substantially better agreement with experiment, and QCISD predicts the observed configuration I to be the more stable by 16 kJ mol^{-1}.[2] Remarkably, the UHF results for HC_3O are more accurate than the B3LYP results obtained with the same basis set.

The CCSD(T) energies further support the QCISD results. In all cases, the QCISD and CCSD(T) relative energies agree to within 3.2 kJ mol^{-1}. The significant qualitative discrepancy in the B3LYP relative energy of the H_2C_2HCO isomers led us further to carry out single-point MP4(SDTQ) energy calculations on those configurations. These results also predict configuration I is more stable than II, by 4.2 kJ mol^{-1}.

3.2. H_2C_2HCO. This lowest energy isomer also possesses the most interesting vibrational surface, plotted along two coordinates in Figure 3. There are three distinct configurations on this surface, all of which are found to be local minima: I (*trans*), Ic (*cis*), and II. The lowest energy path between any two of these isomers has a transition state with the CO bond bent out of the H_2C_3H plane by roughly 40°. Although there could in principle be three transition states on this surface, it appears that instead there is one transition state (barrier = 13.7 kJ mol^{-1}) between the two isomers of configuration I and one additional transition state (barrier = 16.4 kJ mol^{-1}) between the *cis*−*trans* reaction path for I and configuration II.

Selected harmonic vibrational frequencies of all three configurations of H_2C_2HCO are given in Table 2. The lowest frequency mode for each isomer corresponds to the isomerization coordinate, which near the I and Ic stationary points takes the form of an internal rotation of the C_cO bond about the C_bC_c bond axis. The low hindrance of this motion results in the extremely low harmonic frequency of 28 cm^{-1} obtained for the Ic configuration. It must be noted that the lowest frequency

TABLE 3: QCISD/6-311G(d,p) Isomerization energies and barriers with (*E) and without (*E*) Zero-Point Vibrational Energy Corrections for H_2C_2HCO, H_3C_3O, and H_2C_3HO, Measured Relative to the Most Stable Configuration of the Structural Isomer[a]**

	E (kJ mol^{-1})	E^* (kJ mol^{-1})
H_2C_2HCO II	7.6	1.4
H_2C_2HCO Ic	8.0	8.1
H_2C_2HCO ts(I−Ic)	13.7	10.9
H_2C_2HCO ts(I−lI)	16.4	11.3
H_3C_3O I	2.1	2.1
H_2C_3HO II	12.8	14.4
H_2C_3HO ts	13.6	14.5

[a] Zero-point energy corrections neglect the isomerization coordinate.

motions are unlikely to be well-represented by the harmonic oscillator approximation, but we plan to use the potential energy surfaces shown in Figure 3 to obtain more accurate vibrational frequencies.

Based on the harmonic vibrational frequencies, zero-point corrections are applied to the minima and transition states to obtain the corrected relative energies of Table 3. The most significant of these adjustments is the drop in relative energy of configurations I and II from 7.6 kJ mol^{-1} to 1.4 kJ mol^{-1}, suggesting these configurations are nearly isoenergetic on the effective potential energy surface. The barrier between them, 11.3 kJ mol^{-1}, remains high enough that distinct isomers of the two configurations are probably observable. This distinguishes H_2C_2HCO from HC_3O, for which the barrier to isomerization from the secondary structure was only 0.3 kJ mol^{-1} after applying the zero-point correction.[2]

Prospects for the spectroscopic identification of these compounds, based on their predicted properties, are excellent. The strongest vibrational mode in configuration II is predicted to have an infrared intensity of 542 km mol^{-1}, and that predicted for configuration I is 211 km mol^{-1}. Both are stretching transitions in the 1900−2200 cm^{-1} range, where infrared diode lasers are at their best.

The most precise determinations of molecular geometries are made by pure rotational spectroscopy, and here too configuration I is an outstanding candidate for observation. Table 4 lists the QCISD predicted dipole moment components along the *a* and *b* inertial axes. (Because all structures lísted are of C_s symmetry, the *c* component of the dipole moment is zero.) Configuration I has a predicted *a*-axis dipole moment of 3.5 D, and for Ic the prediction is 2.5 D. These configurations should be strong microwave absorbers. Configuration II, having a less polar cumulenic structure, has dipole moment components of 0.86 and 0.65 D, making detection more difficult but still quite feasible.

Carbon-13 Fermi contact hyperfine constants are also listed in Table 4. The hyperfine parameters are extremely sensitive checks of the ab initio calculations and may be measured by rotational spectroscopy of the H_2C_2HCO isotopomers. The significant s electron character of the unpaired electron in configuration I is indicated by the 360−390 MHz C_c hyperfine constants. These values are consistent with the 365 MHz value found for the $H^{13}CO$ Fermi contact term,[21] in which the unpaired electron is in a nearly pure sp^2 hybrid orbital.

3.3. H_3C_3O. Figure 1 gives a misleading representation of the ground electronic state of H_3C_3O. Rather than being ^{2}A′, as the canonical structure II suggests, the molecule is more stable in a ^{2}A″ state. In retrospect, this is consistent with the electronic structure of HCCO,[22] which has a ^{2}A″ ground state and differs from H_3C_3O only in the replacement of the H atom by a methyl group. Canonical structure I is appropriate, save that the unpaired electron favors an out-of-plane a″ p-type orbital to the in-plane a′ sp^2-type orbital. This may be viewed as a Jahn−Teller distortion of a C_{3v} symmetric configuration I, analogous to the Renner−Teller distortion that breaks the degeneracy of the linear HCCO $^2\Pi$ state. The ground electronic state of the C_{3v} form of H_3C_3O I is a doubly degenerate ^2E state, which splits into the more stable ^{2}A″ state and an excited ^{2}A′ state.

That the ^{2}A″ state is more stable can be justified in classical terms by considering the MO configuration of the linear HCCO. The ground state has seven π electrons, giving an occupation of π^3 to the highest energy MO. The linear forms of HCO and HC_3O, in contrast, have five and nine π electrons, respectively, with a single unpaired π electron in the MO configuration. When any of these molecules bends, the partially occupied π orbital splits into an a′ in-plane orbital and an a″ out-of-plane orbital. The a′ orbital is lower in energy because it permits greater nuclear−electronic interaction than the a″, which is constrained to have a nodal plane coinciding with the nuclear plane. For HCCO, the π^3 HOMO configuration becomes a′^{2}a″, making the molecular ground state ^{2}A″. For HCO and HC_3O, the π^1 HOMO configuration becomes a′^{1}, and those molecules have ^{2}A′ ground states.

The H_3C_3O structural isomer was found at all levels of theory to exhibit a single stable geometry. At the UHF level, this geometry was essentially the C_{3v} form of configuration I in Figure 1. At higher levels of theory, the equilibrium geometry has characteristics of both configurations I and II. Indeed, the QCISD optimized CCC bond angle is 150°, halfway between the 120° and 180° bond angles of the canonical geometries. (Note that this molecule foils the traditional chemical nomenclature methods, being poorly approximated as either a propynoxy or a propenonyl radical.) The optimized structure has C_s symmetry, with a *trans* HCCC planar backbone. The QCISD vertical separation between the ground state and ^{2}A′ excited Jahn−Teller state is 610 kJ mol^{-1} at the equilibrium geometry.

In calculations on H_3C_3O, nearly unhindered internal rotation of the methyl group is apparent, leading to extremely slow convergence of the geometry optimization. This characteristic results from the near-single bond character of the C_aC_b bond and the low steric interference of the long carbon chain.

The coexistence of configurations I and II causes the CCCO bending potential energy surface for H_3C_3O to be extremely flat. We modeled the isomerization coordinate between these

TABLE 4: QCISD/6-311G(d,p) Dipole Moments μ (D) and ^{13}C Fermi Contact Terms *a* (MHz) for Configurations of the Three Most Stable C_3H_3O Structural Isomers[a]

	H_2C_2HCO I	H_2C_2HCO Ic	H_2C_2HCO II	H_3C_3O	H_2C_3HO I	H_2C_3HO II
μ_a	−3.49	−2.52	−0.86	−2.51	−2.66	−2.80
μ_b	0.24	−0.28	−0.65	0.76	−1.28	1.47
$a(C_a)$	−69.5	27.1	62.9	−27.8	−53.8	−1.0
$a(C_b)$	227.0	153.4	−53.8	55.5	55.0	348.1
$a(C_c)$	367.6	385.5	16.7	64.4	−51.7	18.7

[a] Dipole moments are taken as pointing from negative to positive, and the *a*- and *b*- axes are defined to be positive towards the O atom.

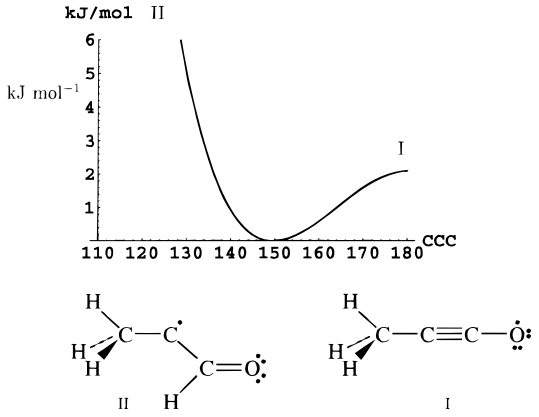

Figure 4. Plot of the effective vibrational potential energy of H_2C_3HO as a function of the CCC bond angle.

two structures by the CCC bond angle and calculated the potential energy at 10° intervals along that path. The results, plotted in Figure 4, show a barrier to linearity of the CCCO chain of 2.1 kJ mol^{-1} or 175 cm^{-1}. Given the harmonic bending frequency of 130 cm^{-1}, this implies that the vibrational spectrum of H_3C_3O will be characteristic of a quasilinear molecule.[23] The zero-point correction based on the harmonic frequencies is less than 20 cm^{-1}.

The unoccupied a′ orbital on the center carbon atom is available for bonding, and it is conceivable that internal hydrogen transfer could occur rapidly between H_3C_3O and any of the more stable H_2C_2HCO isomers. We have investigated this structural isomerization path only at the UHF/6-311G(d,p) level, which predicts an isomerization barrier of 190 kJ mol^{-1} relative to H_3C_3O. Although correlated methods will probably reduce this barrier height, this hydrogen transfer is not a facile isomerization pathway.

Prospects for spectroscopic observation of H_3C_3O are again good. The strongest vibrational transition has a predicted strength of 300 km mol^{-1} and the *a*-axis dipole moment is calculated to be 2.5 D.

3.4. H_2C_3HO. The H_2C_3HO isomers are related to the H_2C_2HCO isomers by reversal of the isoelectronic CH_2 and O groups. Configuration I of H_2C_2HCO in this way resembles configuration II of H_2C_3HO, and vice versa. In this light, it is consistent that H_2C_3HO has potential minima at each of these distinct geometries. These minima appear in the QCISD bending potential surface, shown in Figure 5.

The barrier for isomerization from configuration I to configuration II is 14.5 kJ mol^{-1}, after including zero-point corrections. However, the secondary minimum is only 0.1 kJ mol^{-1} deep, and the transition state is very near the geometry of configuration II. The well for configuration II is so shallow and confined to so narrow a region that it is unlikely to have a substantial impact on the experimental properties of the system. Similarly, the expected H_2C_3HO IIc configuration is not stable at all, that region of the potential energy surface being characterized by a gradual slope rather than a local minimum. Shifts of only a few kilojoules per mole in the relative energies of these structures are sufficient to add or remove configuration II local minima from this surface, and the present calculations are not expected to be accurate to within 2 kJ mol^{-1}. However, the qualitative result of Figure 5 is likely to be reliable: namely, that there is a broad minimum near configuration I with an extremely flat, higher energy region corresponding to the configuration II isomers.

Although the frequencies of the asymmetric carbon stretching transition in each configuration of H_2C_3HO are similar (1870 and 1881 cm^{-1}), the intensities are vastly different: 6.5 and 311 km mol^{-1} respectively for configurations I and II. For hydrocarbon free radicals, the normally reliable frequency range and strength of these transitions make them popular candidates for infrared detection. For this structure, however, the intensity of the transition appears to strongly favor detection of the less stable configuration. Vibrational spectroscopy of the more stable configuration I may be hampered by dissipation of the stretching transition strength over several modes, at 942, 1527, and 3027 cm^{-1}. Rotational spectroscopy of this structure, however, remains feasible with predicted dipole moments of over 2.5 D for both configurations.

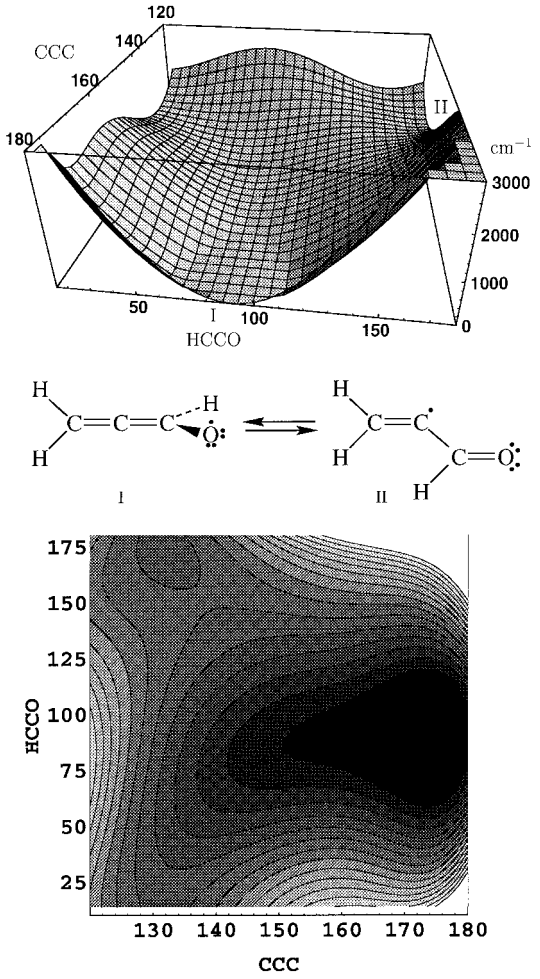

Figure 5. Contour and perspective plots of the effective vibrational potential energy surface of H_2C_3HO as a function of the CCC bond angle and HCCO dihedral angle.

3.5. Other Isomers. The four configurational isomers of HC_2HCHO are all found to be stable and similar in energy to the H_2C_3HO configurations. The isomerization paths for this structure amount to various *cis*−*trans* isomerizations and were not pursued. Harmonic vibrational frequencies were calculated for the tc configuration (*trans*-CCCO, *cis*-HCCC) at the QCISD level to test for anomalously low force constants. The lowest frequency, 139 cm^{-1}, corresponds to internal rotation about the C−C single bond. This rotation, similar to rotation about the C−C bond in the H_2C_2HCO I and Ic configurations, is hindered by the disruption of conjugation between the two π-bonds. The predicted frequency is consistent with the 142 cm^{-1} frequency seen for the analogous motion in H_2C_2HCO I.

The energy ordering of these four configurations is somewhat as anticipated, with the tt and tc isomers, with *trans*-CCCO chains, most stable. Between the two *cis*-CCCO isomers cc

and ct, the ct isomer is less stable despite the expected reduction in steric interaction between the oxygen and terminal hydrogen atoms. However, over the separation distance of 2.9 Å between these two atoms, the steric hindrance may be negligible. The lower energy of the cc isomer relative to ct may be attributable to a favorable electrostatic interaction between the terminal hydrogen atom (QCISD Mulliken charge 0.12*e*) and the oxygen (charge −0.28*e*).

Many other structural isomers of C_3H_3O are possible, although few present the opportunity for relocalization paths seen in the structures already discussed. Those already discussed also constitute the likely kinetically-favored products of hydrogen abstraction from the most stable C_3H_4O isomers, acrolein, methylketene, and 2-propyn-1-ol. Additional UHF/6-311G(d,p) calculations were carried out on nearly all remaining C_3H_3O structural isomers, including the alcohols, three- and four-membered rings, ethers, and several radical carbenes—31 additional structures in all. The lowest energy of these structures, the HC_3HOH propadienolyl radical, lay 33 kJ mol^{-1} higher in energy than the HC_2HCHO cc isomer; all other structures were at least 70 kJ mol^{-1} higher in energy. The qualitative success of the UHF calculations leads us to conclude that H_2C_2HCO, H_3C_3O, H_2C_3HO, and HC_2HCHO are indeed the most stable structural isomers.

4. Conclusions

Isomerization through relocalization of electrons in free radicals has been predicted by the present work to extend beyond the family of HC_3O analogs previously studied to C_3H_3O. Unlike HC_3O, the relocalization isomers in H_2C_2HCO and H_2C_3HO correspond to different electronic states connected via a C_1 transition state. Calculations on these systems obtain useful qualitative results at the UHF level. However, the relative energies of the configurational isomers are less than 15 kJ mol^{-1} and demand high levels of theory for convergence.

The energy ordering of the most stable structural isomers of C_3H_3O is unambiguously predicted to be (in increasing energy) H_2C_2HCO, H_3C_3O, H_2C_3HO, and HC_2HCHO. The highest levels of theory also consistently predict the following: (i) the most stable configuration of all is configuration I of H_2C_2HCO; (ii) H_3C_3O has but a single stable structure, an average of configurations I and II; (iii) configuration I of H_2C_3HO is more stable than configuration II; (iv) the four configurations of HC_2HCHO are all stable, with the *trans*−*trans* configuration the most stable of the group.

If a suitable production mechanism can be found for these species, their rotational spectra should be easily obtained, given the large *a*-axis dipole moment predicted for each configuration. All configurations save H_2C_3HO I are predicted to have strong carbon stretching transitions in the 1800−2200 cm^{-1} interval. Because all configurations studied have a floppy vibrational mode, all are good candidates for hot band or combination band spectra.

With relocalization barriers of less than 15 kJ mol^{-1}, it is quite likely that the three most stable structures of C_3H_3O exist in high-temperature combustion systems only as admixtures of two or more canonical structures. These intermediates may therefore add yet another challenge to modeling of combustion reaction kinetics.

Acknowledgment. These calculations were carried out partly at the Mississippi Center for Supercomputing Research. The author thanks D. Southard, A. Johnson, and E. Cummings for assistance. This work was funded by the National Science Foundation and by the Exxon Education Foundation. Acknowledgment is also made to the donors of The Petroleum Research Fund, administered by the ACS, for partial support of this research.

Supporting Information Available: Tables listing all stationary point vibrational frequencies, QCISD $\langle S^2 \rangle$ and MCSCF c_0 values, and bond lengths and bond angles for UHF, B3LYP, and MCSCF levels of theory (5 pages). Ordering information is given on any current masthead page.

References and Notes

(1) Cooksy, A. L. *J. Am. Chem. Soc.* **1995**, *117*, 1098.
(2) Cooksy, A. L.; Tao, F.-M.; Klemperer, W.; Thaddeus, P. *J. Phys. Chem.* **1995**, *99*, 11095.
(3) Wang, H.; Cooksy, A. L. *Chem. Phys.* **1996**, *213*, 139.
(4) Bouchoux, G.; Hoppilliard, Y.; Flament, J. P. *Org. Mass Spectrom.* **1985**, *20*, 560−564.
(5) Martynov, S. N.; Gurevich, R. I. *Izv. Akad. Nauk Resp. Kaz., Ser. Khim.* **1992**, *3*, 31−34.
(6) Irvine, W. M.; et al. *Astrophys. J.* **1988**, *335*, L89−L93.
(7) Adams, N. G.; Smith, D.; Giles, D. K.; Herbst, E. *Astron. Astrophys.* **1989**, *220*, 269−271.
(8) Scott, G. B. I.; Fairley, D. A.; Freeman, C. G.; R. G. A. R. Maclagan, M. J. M. *Int. J. Mass Spectrom. Ion Processes* **1995**, *149/150*, 251−255.
(9) Petrie, S. *Astrophys. J.* **1995**, *454*, L165−L168.
(10) Schmidt, M. W.; et al. *J. Comput. Chem.* **1993**, *14*, 1347−1363.
(11) Frisch, M. J.; et al. *Gaussian 94*, Revision C; Gaussian, Inc.: Pittsburgh, PA, 1994.
(12) Krishnan, R.; Binkley, J. S.; Seeger, R.; Pople, J. A. *J. Chem. Phys.* **1980**, *72*, 650−654.
(13) Frisch, M. J.; Pople, J. A.; Binkley, J. S. *J. Chem. Phys.* **1984**, *80*, 3265−3269.
(14) Werner, H.-J. *Adv. Chem. Phys.* **1987**, *69*, 1−62.
(15) Pipek, J.; Mezey, P. Z. *J. Chem. Phys.* **1989**, *90*, 4916−4926.
(16) Pople, J. A.; Head-Gordon, M.; Raghavachari, K. *J. Chem. Phys.* **1987**, *87*, 5968−5975.
(17) Krishnan, R.; Pople, J. A. *Int. J. Quantum Chem.* **1978**, *14*, 91−100.
(18) Becke, A. D. J. *Chem. Phys.* **1993**, *98*, 5648−5652.
(19) Lee, C.; Yang, W.; Parr, R. G. *Phys. Rev. B* **1988**, *37*, 785−789.
(20) Müller, H.; Kutzelnigg, W.; Noga, J.; Klopper, W. *J. Chem. Phys.* **1997**, *106*, 1863−1869.
(21) Holmberg, R. W. *J. Chem. Phys.* **1969**, *51*, 3255−3260.
(22) Szalay, P. G.; Stanton, J. F.; Bartlett, R. *J. Chem. Phys. Lett.* **1992**, *193*, 573−579.
(23) Winnewisser, B. P. In *Molecular Spectroscopy: Modern Research*; Rao, K. N., Ed.; Academic Press: Orlando, FL, 1985; Vol. III.